

# Stochastic Modeling of Fatigue Crack Damage for Risk Analysis and Remaining Life Prediction<sup>1</sup>

Asok Ray

Mechanical Engineering Department,  
The Pennsylvania State University,  
University Park, PA 16802  
Fellow ASME  
e-mail: axr2@psu.edu

*This paper presents a stochastic model of fatigue crack damage in metallic materials that are commonly encountered in structures and machinery components of complex mechanical systems (e.g., aircraft, spacecraft, and power plants). The constitutive equation of the damage model is based on the physics of fracture mechanics and is validated by Karhunen-Loève analysis of test data. The (nonstationary) probability distribution function (PDF) of fatigue crack damage is generated in a closed form without numerically solving stochastic differential equations in the Wiener integral or Itô integral setting. The crack damage model thus allows real-time execution of decision algorithms for risk assessment and life prediction on inexpensive platforms such as a Pentium processor. The model predictions are in close agreement with experimental data of fatigue crack growth statistics for 2024-T3 and 7075-T6 aluminum alloys.*

## 1 Introduction

Traditionally, the risk index and remaining service life (Bolotin, 1989) of machinery are calculated off-line based on statistical models of material degradation, operating history and anticipated disruptions in the plant operation (e.g., postulated stress levels). Since the predicted service life of an operating machinery is likely to be altered in the event of unscheduled operations, on-line computation of damage statistics allows continual refinement of the risk index and remaining life prediction as time progresses. In this context, this paper focuses on stochastic modeling of fatigue crack damage in metallic materials, which is a major source of failures in structural components of operating machinery (Özekici, 1996).

Stochastic modeling of fatigue crack phenomena in ductile alloys is a relatively new area of research, and a list of the literature representing the state of the art is cited by Sobczyk and Spencer (1992) as well as in the March, 1996 issue of *Engineering Fracture Mechanics*. Bogdonoff and Kozin (1985) proposed a Poisson-like independent-increment jump model of fatigue crack phenomena. The underlying principle of this model agrees with the theory of micro-level fatigue cracking. An alternative approach to stochastic modeling of fatigue crack damage is to randomize the coefficients of an existing deterministic model to represent material inhomogeneity (Ditlevsen, 1986). Another alternative approach is to augment a deterministic model of fatigue crack growth with a random process (Lin and Yang, 1985; Spencer et al., 1989; Ishikawa et al., 1993, for example). The fatigue crack growth process is thus modeled by nonlinear stochastic differential equations in the Itô setting (Kloeden and Platen, 1995). Specifically, Kolmogorov forward and backward diffusion equations, which require solutions of nonlinear partial differential equations, have been proposed to generate the statistical information required for risk analysis of mechanical structures (Tsurui and Ishikawa, 1986; Bolotin, 1989). These nonlinear partial differential equations can only be solved numerically and the numerical procedures are computationally

intensive as they rely on fine-mesh models using finite-element or combined finite-difference and finite-element methods (Sobczyk and Spencer, 1992). Casciati et al. (1992) have analytically approximated the solution of Itô equations by Hermite moments to generate a probability distribution function of the crack length.

This paper presents a stochastic model of fatigue crack damage in metallic materials that are commonly encountered in structures and machinery components of complex mechanical systems (e.g., aircraft, spacecraft, and power plants). The fatigue crack damage at an instant (i.e., at the end of a stress cycle) is expressed as a continuous function of the current and initial crack lengths. The (nonstationary) probability distribution of crack damage is obtained in a closed form without numerically solving stochastic differential equations in the Wiener integral or Itô integral setting. Model predictions are shown to be in close agreement with the fatigue test data of 2024-T3 and 7075-T6 aluminum alloys. The paper also illustrates how the stochastic model can be used in making decisions for risk analysis and life prediction that are necessary for health management and life extending control of mechanical systems. The paper is organized in four sections including the introduction. Section 2 provides details of model formulation, identification of the model parameters, and their probability distributions along with the results of model prediction. Section 3 deals with risk analysis and remaining life prediction. The paper is summarized and concluded in Section 4 with recommendations for future research.

## 2 Modeling of Fatigue Crack Damage

Fatigue crack growth models have been formulated by fitting estimated mean values of fatigue crack length, generated from ensemble averages of experimental data, as functions of time in units of cycles (Paris and Erdogan, 1963; Schjive, 1976). Following Sobczyk and Spencer (1992) and the pertinent references cited therein, the stochastic model of fatigue crack damage, presented in this paper, is built upon the structure of the following mean-value model (Anderson, 1995; Suresh, 1991):

$$\delta \hat{c}(t) = h(\Delta K_{\text{eff}}(t)) \delta t; \quad \text{for } t \geq t_0 \quad \text{and given } \hat{c}(t_0)$$

$$\Delta K_{\text{eff}}(t) = \Delta S(t) \sqrt{\pi \hat{c}(t)} F(\hat{c}(t))$$

$$\Delta S(t) = S^{\max}(t) - S^o(t) \quad (1)$$

where  $t$  is the current time upon completion of a stress cycle, and  $t_0$  is the initial time (e.g., when the machine component is put in

<sup>1</sup>The research work reported in this paper is supported in part by: National Science Foundation under Grant No. DMI-9424587; National Science Foundation under Grant No. CMS-9531835; NASA Langley Research Center under Grant No. NCC-1-249; National Academy of Sciences under a Research Fellowship award.

Contributed by the Dynamic Systems and Control Division for publication in the *JOURNAL OF DYNAMIC SYSTEMS, MEASUREMENT, AND CONTROL*. Manuscript received by the Dynamic Systems and Control Division August 13, 1997; revised manuscript received May 1, 1999. Associate Technical Editor: S. D. Fassois.

service after a major maintenance or inspection);  $\hat{c}(t)$  is the estimated mean value of (time-dependent) crack length;  $\delta\hat{c}(t)$  is the increment of the estimated mean crack length over one cycle after time  $t$ , and  $\delta t$  indicates the time increment over that cycle;  $h(\cdot)$  is a non-negative continuous function which is dependent on the material and geometry of the stressed component; and  $\Delta S(t)$  is the effective stress range during one cycle (after time  $t$ ) with the corresponding crack opening stress  $S^o(t)$  and peak stress  $S^{\max}(t)$ . The (dimensionless) correction factor  $F$  is dependent on geometrical configuration (e.g., thickness, width, and the crack type in the stressed component) and the crack length. For example,  $F = \sqrt{\sec(\pi\hat{c}(t)/(2w))}$  for center-cracked specimens of half-width  $w$ . There are several empirical and semi-empirical methods (e.g., Newman, 1984) for calculating  $S^o$ . For constant-amplitude load, Ibrahim et al. (1986) have formulated a simple algebraic relation to obtain  $S^o$  as a function of peak stress  $S^{\max}$  and stress ratio  $R \equiv S^{\min}/S^{\max}$ .

It has been shown in the fracture mechanics literature (Anderson, 1995; Suresh, 1991) that, for a given geometry (i.e., thickness and width) of center-cracked specimens, the function  $h(\cdot)$  is separable as a product of two functions,  $h_1(\Delta S(t))$  and  $h_2(\hat{c}(t))$ . Accordingly, for center-cracked specimens with  $0 < \hat{c}(t) \ll w \forall t \geq t_o$ , Eq. (1) is modified via series approximation of the  $(m/2)^{\text{th}}$  power of the secant term in the correction factor  $F$  as:

$$\delta\hat{c}(t) = \hat{\Omega}\Delta S(t)^m \hat{c}(t)^{m/2} \left(1 - m\left(\frac{\pi}{4w}\right)^2 \hat{c}(t)^2\right)^{-1} \delta t; \quad t \geq t_o \text{ and given } \hat{c}(t_o) \quad (2)$$

where the constant parameters  $\hat{\Omega}$  and  $m$  are dependent on the specimen material, geometry, and fabrication. For constant-amplitude load, Eq. (2) reduces to the well-known Paris equation (Suresh, 1991). For varying-amplitude load, Patankar et al. (1998) have shown the validity of Eq. (2) under time-dependent stress range  $\Delta S(t) \equiv (S^{\max}(t) - S^o(t))$  by having  $S^o(t)$  as a state variable.

Ditlevsen (1986) has shown that, under constant load amplitude, the randomness of fatigue crack growth accrues primarily from parametric uncertainties. The stochastic process of crack growth is largely dependent on two second-order random parameters—a multiplicative process  $\Omega(\zeta, \Delta S)$  and an exponent parameter  $m(\zeta)$ . Ditlevsen (1986) has suggested the possibility of one of the above two random variables being a constant for all specimens  $\zeta$ . Statistical analysis of the experimental data for 2024-T3 and 7075-T6 aluminum alloys reveals that the random exponent  $m(\zeta)$  can be approximated as a constant for all specimens (i.e.,  $m(\zeta) = m$  with probability 1) at different levels of constant stress range  $\Delta S$  for a given material. Based on this observation and the (deterministic) model structure in Eq. (2), we postulate the following constitutive equation for fatigue crack growth in the stochastic setting (Sob-

czyk and Spencer, 1992) partly similar to what was originally proposed by Paris and Erdogan (1963) in the deterministic setting:

$$\delta c(\zeta, t) = \Omega(\zeta, \Delta S(t)) (\Delta S(t))^m c(\zeta, t)^{m/2} \times \left(1 - m\left(\frac{\pi}{4w}\right)^2 c(\zeta, t)^2\right)^{-1} \rho(\zeta, t) \delta t; \quad t \geq t_o \text{ and given } c(\zeta, t_o) \quad (3)$$

where the second order random process  $\Omega(\zeta, \Delta S)$  represents uncertainties of a test specimen  $\zeta$  for a stress range  $\Delta S$  (i.e.,  $\Omega$  is a constant for a given specimen under a constant stress range); the second order noise process  $\rho(\zeta, t)$  represents uncertainties in the material microstructure and crack length measurements that vary with crack propagation even for the same specimen  $\zeta$ . The multiplicative uncertainty  $\rho(\zeta, t)$  in the crack growth process is assumed to be a stationary white noise process that is statistically independent of  $\Omega(\zeta, \Delta S)$ . The rationale for this assumption is that inhomogeneity of the material microstructure and measurement noise associated with each test specimen, represented by  $\rho(\zeta, t)$ , are statistically homogeneous and are unaffected by the uncertainty  $\Omega(\zeta, \Delta S)$  of a particular specimen caused by, for example, machining operations. With no loss of generality,  $\mu_\rho \equiv E[\rho(\zeta, t)] = 1$  is set via appropriate scaling of the parameters in Eq. (3).

Since the number of cycles to failure is usually very large in the crack growth processes (even for low-cycle fatigue), a common practice in the fracture mechanics literature is to approximate the difference equation of crack growth by a differential equation. Therefore, for  $t \geq t_o$ , Eq. (3) is approximated as the following stochastic differential equation:

$$\left((c(\zeta, t))^{-m/2} - m\left(\frac{\pi}{4w}\right)^2 (c(\zeta, t))^{2-m/2}\right) dc(\zeta, t) = \Omega(\zeta, \Delta S(t)) (\Delta S(t))^m \rho(\zeta, t) dt; \quad t \geq t_o \text{ and given } c(\zeta, t_o) \quad (4)$$

which is integrated pointwise (i.e., for the individual  $\zeta$ 's) as follows:

$$\int_{c(\zeta, t_o)}^{c(\zeta, t)} \frac{d\xi}{\xi^{m/2}} - m\left(\frac{\pi}{4w}\right)^2 \int_{c(\zeta, t_o)}^{c(\zeta, t)} \frac{d\xi}{\xi^{-2+m/2}} = \int_{t_o}^t d\tau (\Delta S(\tau))^m \Omega(\zeta, \Delta S(\tau)) \rho(\zeta, \tau); \text{ given } c(\zeta, t_o) \quad (5)$$

to yield the following (almost sure) solution

## Nomenclature

$C$ = autocovariance; covariance matrix	$R$ = stress ratio ( $S^{\min}/S^{\max}$ ); autocorrelation	$\xi$ = dummy variable
$c$ = crack length	$S$ = stress	$\Lambda$ = (diagonal) eigenvalue matrix
$\bar{c}_M$ = critical crack length	$T$ = maximum time of operation	$\lambda$ = eigenvalue
$\bar{c}_o$ = threshold of initial crack length	$t$ = time (cycles)	$\mu$ = expected value
$F(\cdot)$ = probability distribution function (PDF)	$X$ = random vector	$\rho$ = multiplicative white noise
$f$ = final condition	$x$ = random variable	$\sigma$ = standard deviation
$H$ = hypothesis	$Y_d$ = desired operational profile	$\tau$ = dummy variable
$K$ = stress intensity factor	$\Delta$ = incremental range	$\Psi$ = discretized fatigue crack damage
$M$ = number of hypotheses	$\delta$ = increment operator	$\psi$ = continuous fatigue crack damage
$m$ = exponent parameter of the model	$\delta(\cdot)$ = unit impulse function	$\Omega$ = multiplicative parameter of the model
$o$ = initial condition; opening condition	$1 - \epsilon$ = confidence level for risk analysis	$\zeta$ = sample point (test specimen)
$P[\cdot]$ = probability measure	$\phi$ = eigenvector	

$$\left( \frac{c(\zeta, t)^{1-m/2} - c(\zeta, t_0)^{1-m/2}}{1 - \frac{m}{2}} \right) - m \left( \frac{\pi}{4w} \right)^2 \left( \frac{c(\zeta, t)^{3-m/2} - c(\zeta, t_0)^{3-m/2}}{3 - \frac{m}{2}} \right) = \int_{t_0}^t d\tau \Omega(\zeta, \Delta S(\tau)) (\Delta S(\tau))^m \rho(\zeta, \tau) \quad (6)$$

where the constant parameter,  $m$ , is in the range of 2.5 to 5 for ductile alloys and many metallic materials ensuring that  $(1 - m/2) < 0$  and  $(3 - m/2) > 0$  in Eq. (6). Now we introduce a stochastic process  $\psi(\zeta, t; t_0)$  to represent the (dimensionless) fatigue crack damage as a function of the crack length  $c(\zeta, t)$  after normalization relative to the physical parameter,  $w$ , of the stressed specimen:

$$\psi(\zeta, t; t_0) \equiv \left( \left( \frac{c(\zeta, t)^{1-m/2} - c(\zeta, t_0)^{1-m/2}}{1 - \frac{m}{2}} \right) - m \left( \frac{\pi}{4w} \right)^2 \left( \frac{c(\zeta, t)^{3-m/2} - c(\zeta, t_0)^{3-m/2}}{3 - \frac{m}{2}} \right) \right) w^{(m/2)-1} = \left( \frac{(c(\zeta, t)/w)^{1-m/2} - (c(\zeta, t_0)/w)^{1-m/2}}{1 - \frac{m}{2}} \right) - m \left( \frac{\pi}{4} \right)^2 \left( \frac{(c(\zeta, t)/w)^{3-m/2} - (c(\zeta, t_0)/w)^{3-m/2}}{3 - \frac{m}{2}} \right) \quad (7)$$

It follows from Eq. (7) that  $\psi(\zeta, t; t_0)$  is a continuous function of the crack length process  $c(\zeta, t)$ . Since  $c(\zeta, t)$  is a measurable function,  $\psi(\zeta, t; t_0)$  is also a measurable function although the two measure spaces are different. The probability distribution of  $\psi(\zeta, t; t_0)$ , conditioned on the initial crack length  $c(\zeta, t_0)$ , leads to a measure of fatigue crack damage at the instant  $t$ . The conditional probability distribution  $F_{\psi(\zeta, t_0)}(\cdot; t)$  that depends on the stress history  $\{\Delta S(\tau): \tau \in [t_0, t]\}$  plays an important role in risk analysis and remaining life prediction as illustrated later by an example in Section 3.

Next let us consider the special case of constant stress range  $\Delta S$  for which experimental data of random fatigue are available for model validation and parameter identification. A combination of Eqs. (6) and (7) yields the following simplified relation for constant  $\Delta S$ :

$$(\zeta, t; t_0) = w^{(m/2)-1} (\Delta S)^m \Omega(\zeta, \Delta S) \times \left( t - t_0 + \int_{t_0}^t d\tau (\rho(\zeta, \tau) - 1) \right) \quad \text{with probability 1} \quad (8)$$

Given that  $E[\rho(\zeta, t)] = 1$ ;  $E[(\rho(\zeta, t_1) - 1)(\rho(\zeta, t_2) - 1)] = \sigma_\rho^2 \delta(t_1 - t_2)$ ;  $m(\zeta) = m$  with probability 1; and  $\rho(\zeta, t)$  is statistically independent of  $\Omega(\zeta, \Delta S)$ , it follows from Eq. (8) that:

$$\mu_\psi(t; t_0) \equiv E[\psi(\zeta, t; t_0)] = w^{(m/2)-1} (\Delta S)^m \mu_\Omega(\Delta S) (t - t_0) \quad (9)$$

$$R_{\psi\psi}(t_1, t_2; t_0) \equiv E[\psi(\zeta, t_1; t_0) \psi(\zeta, t_2; t_0)] = w^{m-2} (\Delta S)^{2m} (\mu_\Omega^2(\Delta S) + \sigma_\Omega^2(\Delta S)) ((t_1 - t_0)(t_2 - t_0) + \sigma_\rho^2 (\min(t_1, t_2) - t_0)) \quad (10)$$

where  $\mu_\Omega(\Delta S) \equiv E[\Omega(\zeta, \Delta S)]$  and  $\sigma_\Omega^2(\Delta S) \equiv \text{Var}[\Omega(\zeta, \Delta S)]$ . The autocorrelation function  $R_{\psi\psi}(t_1, t_2; t_0)$  in Eq. (10) is continuous at  $(t_1, t_2) |_{t_1=t_2=t}$  for all  $t \geq t_0$ . Hence, the process  $\psi(\zeta, t; t_0)$  is mean-square continuous based on a standard theorem of mean-square calculus (Jazwinski, 1970; Wong and Hajek, 1985).

*Remark:* An examination of Eqs. (4) to (8) reveals that the modeled process  $\psi(\zeta, t; t_0)$  is also almost surely continuous due to the approximation of the difference Eq. (3) by the differential Eq. (4). However, in the sequel, we only require mean-square continuity of  $\psi(\zeta, t; t_0)$  to analyze discrete experimental data. Bogdonoff and Kozin (1985) have represented the crack propagation process by a Poisson-like Markov jump model that is mean-square (but not almost surely) continuous. Similar results were also experimentally obtained by Kogajev and Liebedinskij (1983). Ray and Tangirala (1997) and Ray et al. (1998) have validated the postulation that the autocovariance function of fatigue crack length is continuous by testing four different sets of experimental data of random fatigue.

It follows from Eqs. (9) and (10) that the autocovariance function of  $\psi(\zeta, t; t_0)$  for constant  $\Delta S$  is:

$$C_{\psi\psi}(t_1, t_2; t_0) = w^{m-2} (\Delta S)^{2m} (\sigma_\Omega^2(\Delta S) (t_1 - t_0)(t_2 - t_0) + (\mu_\Omega^2(\Delta S) + \sigma_\Omega^2(\Delta S)) \sigma_\rho^2 (\min(t_1, t_2) - t_0)) \Rightarrow \sigma_\psi^2(t; t_0) \equiv \text{Var}[\Psi(\zeta, t; t_0)] = w^{m-2} (\Delta S)^{2m} \sigma_\Omega^2(\Delta S) \times (t - t_0)^2 \left( 1 + \frac{\mu_\Omega^2(\Delta S) + \sigma_\Omega^2(\Delta S)}{\sigma_\Omega^2(\Delta S)} \frac{\sigma_\rho^2}{(t - t_0)} \right) \quad \text{for } t > t_0 \quad (11)$$

Having established mean-square continuity of the fatigue crack damage model in Eq. (8), we proceed to justify the postulation of the model structure laid out in the constitutive Eq. (3). To this end, we analyze four experimental data sets of random fatigue via Karhunen-Loève expansion (Wong and Hajek, 1985; Fukunaga, 1990) in Section 2.1. We also use these experimental data sets to identify the model parameters in Section 2.2.

**2.1 Analysis of Experimental Data Via Karhunen-Loève Expansion.** This subsection analyzes fatigue test data via Karhunen-Loève (K-L) expansion (Fukunaga, 1990) to justify postulation of the model structure in Eqs. (3) and (4). We have used experimental data of random fatigue crack growth in 2024-T3 aluminum alloy (Virkler et al., 1979) and 7075-T6 aluminum alloy (Ghonem and Dore, 1987) for which the tests were conducted under different constant load amplitudes at ambient temperature. The Virkler data set was generated for 68 center-cracked specimens (of half-width  $w = 76.2$  mm) at a single constant-amplitude load amplitude with peak nominal stress of 60.33 MPa (8.75 ksi) and stress ratio  $R \equiv S_{\min}/S_{\max} = 0.2$  for about 200,000 cycles; the resulting  $\Delta S \equiv (S^{\max} - S^0) = 21.04$  MPa. The Ghonem data sets were generated for 60 center-cracked specimens each (of half-width  $w = 50.8$  mm) at three different constant load amplitudes: (i) Set 1 with peak nominal stress of 70.65 MPa (10.25 ksi) and  $R = 0.6$  for 54,000 cycles, and the resulting  $\Delta S = 15.84$  MPa; (ii) Set 2 with peak nominal stress of 69.00 MPa (10.00 ksi) and  $R = 0.5$  for 42,350 cycles, and the resulting  $\Delta S = 17.80$  MPa; and (iii) Set 3 with peak nominal stress of 47.09 MPa (6.83 ksi) and  $R = 0.4$  for 73,500 cycles, and the resulting  $\Delta S = 13.24$  MPa. The crack opening stress  $S^0$  is calculated via the correlation of Ibrahim et al. (1986).

Since only finitely many data points at  $l$  discrete instants of time are available from experiments, an obvious choice is discretization over a finite horizon  $[t_0, t_f]$  so that the stochastic process  $\psi(\zeta, t; t_0)$  now reduces to an  $l$ -dimensional random vector denoted as  $\Psi^D(\zeta)$ . Consequently, the covariance function  $C_{\psi\psi}(t_1; t_2; t_0)$  in Eq. (11) is reduced to a real positive-definite ( $l \times l$ ) symmetric matrix  $C_{\Psi\Psi}^D$ . Since the experimental data were taken at sufficiently

close intervals,  $C_{\Psi\Psi}^D$  contains pertinent information of the crack damage process. The  $l$  real positive eigenvalues are ordered as  $\lambda_1 \geq \lambda_2 \geq \dots \geq \lambda_l$ , with the corresponding eigenvectors,  $\phi^1, \phi^2, \dots, \phi^l$ , that form an orthonormal basis for signal decomposition. The K-L expansion also ensures that the  $l$  random coefficients of the basis vectors are statistically orthogonal (i.e., zero-mean and mutually uncorrelated). These random coefficients form a random vector  $X(\zeta) \equiv [x_1(\zeta) \ x_2(\zeta) \ \dots \ x_l(\zeta)]^T$  having the covariance matrix  $C_{XX} = \text{diag}(\lambda_1, \lambda_2, \dots, \lambda_l)$  leading to decomposition of the discretized signal as:

$$\Psi^D(\zeta) = E[\Psi^D(\zeta)] + \sum_{j=1}^l (\phi^j x_j(\zeta)) \quad (12)$$

It was observed by Ray and Tangirala (1997) and Ray et al. (1998) that the statistics of crack length are dominated by the random coefficient corresponding to the principal eigenvector (i.e., the eigenvector associated with the largest eigenvalue) and that the combined effects of the remaining eigenvectors are small. Therefore, the signal  $\Psi^D(\zeta)$  in Eq. (12) is expressed as the sum of a principal part and a residual part:

$$\Psi^D(\zeta) = \underbrace{\Psi^D(\zeta)}_{\text{principal part}} + \underbrace{\sum_{j=2}^l (\phi^j x_j(\zeta))}_{\text{residual part}} \quad (13)$$

If the random vector  $\Psi^D(\zeta)$  is approximated by the principal part

$$\hat{\Psi}^D(\zeta) \equiv E[\Psi^D(\zeta)] + \phi^1 x_1(\zeta), \quad (14)$$

then the resulting (normalized) mean square error (Fukunaga, 1990) is:

$$\begin{aligned} \epsilon_{\text{rms}}^2 &\equiv \text{Trace}(\text{Cov}[(\Psi^D(\zeta) - \hat{\Psi}^D(\zeta))]) / \text{Trace}(\text{Cov}[\Psi^D(\zeta)]) \\ &= \left( \sum_{j=2}^l \lambda_j \right) / \left( \sum_{j=1}^l \lambda_j \right) \end{aligned} \quad (15)$$

The K-L expansion of fatigue test data shows that  $\epsilon_{\text{rms}}^2$  in Eq. (15) is in the range of 0.018 to 0.035 for all four data sets. Furthermore, the principal eigenvector  $\phi^1$ , associated with the largest eigenvalue  $\lambda_1$ , closely fits the ramp function  $(t - t_o)$  in each case and the proportionality constants are directly related to the parameter  $\sigma_{\Omega}^2(\Delta S)$  in Eq. (11) for the respective values of  $\Delta S$  for the individual data sets. Ditlevsen (1986) also observed somewhat similar properties by statistical analysis. Nevertheless, the K-L expansion provides deeper physical insight as seen below.

The terms on the right hand side of Eq. (13) are compared with those of Eq. (8) to generate the following equivalence between the discrete-time model from test data and the postulated continuous-time model:

$$\phi^1 x_1(\zeta) \sim \{(\Delta S)^m (\Omega(\zeta, \Delta S) - \mu_{\Omega}(\Delta S))(t - t_o) : t \in [t_o, t_f]\} \quad (16)$$

$$\sum_{j=2}^l (\phi^j x_j(\zeta))$$

discrete-time model  
derived from test data

$$\sim \left\{ ((\Delta S)^m \Omega(\zeta, \Delta S)) \int_{t_o}^t d\tau (\rho(\zeta, \tau) + 1) : t \in [t_o, t_f] \right\} \quad (17)$$

postulated continuous-time model

Note that the entities in Eqs. (16) and (17) are mutually statistically orthogonal. It follows from Eq. (11) that the uncertainties associated with an individual sample resulting from  $\Omega(\zeta, \Delta S)$  dominate

the cumulative effects of material inhomogeneity and measurement noise due to  $\int_{t_o}^{t_f} d\tau (\rho(\zeta, \tau) - 1)$  unless  $(t_f - t_o)$  is very small. Therefore, from the perspectives of risk analysis and remaining life prediction where  $(t_f - t_o)$  is expected to be large, an accurate identification of the parameters,  $\mu_{\Omega}(\Delta S)$  and  $\sigma_{\Omega}^2(\Delta S)$  of the random process  $\Omega(\zeta, \Delta S)$  is crucial while the role of  $\rho(\zeta, t)$  is much less significant. This observation is consistent with the statistical analysis of fatigue test data by Ditlevsen (1986) where the random process described by Eq. (17) is treated as the zero-mean residual.

**2.2 Identification of Model Parameters and Probability Distributions.** The model parameters,  $m$ ,  $\mu_{\Omega}$ ,  $\sigma_{\Omega}^2$ , and  $\sigma_p^2$ , in Eqs. (9) and (10) are identified based on the four data sets described earlier. The exponent parameter,  $m$ , is first identified as an ensemble average estimate from the slope of the logarithm of crack growth rate in Eq. (3) for both materials, 7075-T6 and 2024-T3. Having known the exponent parameter  $m$ , a database for the random process  $\Omega(\zeta, \Delta S)$  is generated following Eq. (6) over a period  $[t_o, t_f]$  as:

$$\begin{aligned} \Omega(\zeta, \Delta S) &= \frac{\left( \frac{c(\zeta, t)^{1-m/2} - c(\zeta, t_o)^{1-m/2}}{1 - \frac{m}{2}} \right) - m \left( \frac{\pi}{4w} \right)^2 \left( \frac{c(\zeta, t)^{3-m/2} - c(\zeta, t_o)^{3-m/2}}{3 - \frac{m}{2}} \right)}{\left( (t_f - t_o) + \int_{t_o}^{t_f} d\tau (\rho(\zeta, \tau) - 1) \right) (\Delta S)^m} \end{aligned} \quad (18)$$

Given that  $\Omega(\zeta, \Delta S)$  is not explicitly dependent on time by construction of Eq. (4) and  $E[\rho(\zeta, \tau) - 1] = 0$ , the parameter  $\mu_{\Omega}(\Delta S)$  is identified as the ensemble average estimate from the data sets for each type of material, 7075-T6 and 2024-T3 alloys. Since the parameters  $\sigma_{\Omega}^2(\Delta S)$  and  $\sigma_p^2$  cannot be separately identified from Eq. (18) alone, we use the additional information of the eigenvalues,  $\lambda_1, \lambda_2, \dots, \lambda_l$ , of  $C_{\Psi\Psi}^D$  generated by Karhunen-Loève analysis. Taking expected values of Euclidean norms of the terms on both sides of Eqs. (16) and (17) and making use of Eq. (15), we obtain the following relations based on the experimental data over a period  $[t_o, t_f]$ :

$$\text{Var}[(\Delta S)^m \Omega(\zeta, \Delta S)](t_f - t_o)^2 \approx \lambda_1 \Rightarrow \sigma_{\Omega}^2(\Delta S) \approx \frac{(\Delta S)^{-2m} \lambda_1}{(t_f - t_o)^2} \quad (19)$$

$$\begin{aligned} (\Delta S)^{2m} (\sigma_{\Omega}^2(\Delta S) + \mu_{\Omega}^2(\Delta S)) \sigma_p^2 (t_f - t_o) &\approx \sum_{j=2}^l \lambda_j \Rightarrow \frac{\sigma_p^2}{t_f - t_o} \\ &\approx \frac{\sum_{j=2}^l \lambda_j}{\lambda_1 + ((t_f - t_o)(\Delta S)^m \mu_{\Omega}(\Delta S))^2} < \frac{\epsilon_{\text{rms}}^2}{1 - \epsilon_{\text{rms}}^2} \end{aligned} \quad (20)$$

The parameters  $\mu_{\Omega}$ ,  $\sigma_{\Omega}^2$ , and  $\sigma_p^2$  are evaluated via Eqs. (18), (19), and (20) for different ranges of fatigue crack data (i.e., different values of  $t_o$  and  $t_f$ ). The results are consistent for modest changes in  $t_o$  and  $t_f$  confirming that  $\Omega(\zeta, \Delta S)$  is a random variable for a given constant  $\Delta S$  and that  $\rho(\zeta, t)$  is a stationary white noise. Testing with large changes in  $t_o$  and  $t_f$  could not be accommodated because of the limited ranges of sample paths in the experimental data sets.

The following generalized parametric relations are now postulated for different levels of (constant-amplitude) stress excitation for a given material:

- $\mu_{\Omega}(\Delta S) \equiv E[\Omega(\zeta, \Delta S)]$  is independent of  $\Delta S$ , i.e.,  $\mu_{\Omega}$  is a constant and  $E[(\Delta S)^m \Omega(\zeta, \Delta S)] = (\Delta S)^m \mu_{\Omega}$ .
- $\sigma_{\Omega}^2(\Delta S) \equiv \text{Var}[\Omega(\zeta, \Delta S)]$  is proportional to  $(\Delta S)^{-2m}$ , i.e.,  $\text{Var}[(\Delta S)^m \Omega(\zeta, \Delta S)]$  is a constant.

**Table 1 Generalized model parameters based on Virkler et al. and Ghonem and Dore data**

Data Set and Material Type	Stress Range $\Delta S$ (MPa)	$m$ (dimensionless)	$\mu_\Omega$ (SI units)	$(\Delta S)^m \sigma_\Omega / \mu_\Omega$ (SI units)	$\mu_\rho$ (dimensionless)	$(\Delta S)^m \sigma_\rho / \mu_\rho$ (SI units)
Virkler Data 2024-T3 Al	21.04	3.4	$6.4 \times 10^{-7}$	$5.634 \times 10^4$	1.0	$4.980 \times 10^2$
Ghonem Data #1 7075-T6 Al	13.84	3.6	$7.7 \times 10^{-7}$	$7.573 \times 10^4$	1.0	$8.426 \times 10^2$
Ghonem Data #2 7075-T6 Al	17.80	3.6	$7.7 \times 10^{-7}$	$7.573 \times 10^4$	1.0	$8.426 \times 10^2$
Ghonem Data #3 7075-T6 Al	13.24	3.6	$7.7 \times 10^{-7}$	$7.573 \times 10^4$	1.0	$8.426 \times 10^2$

- $\text{Var} [(\Delta S)^m \int_{t_0}^t d\tau (\rho(\zeta, \tau) - 1)]$  is small compared to  $\text{Var} [(\Delta S)^m \Omega(\zeta)(t - t_0)]$  for large  $(t - t_0)$ .

The above three relations are consistent with the experimental data sets of Ghonem and Dore (1987) for 7075-T6 aluminum alloy. The third relation follows from Eq. (11) that provides an approximation for risk analysis and remaining life prediction in Section 3. The first two relations are not yet verified for 2024-T3 aluminum alloy because the Virkler data set provides only one level of stress range. These relations are expected to be valid for ductile alloys and many other metallic materials because the nature of dependence of the model parameters on the material microstructure and specimen preparation (i.e., machining operations) is similar. Estimates of the model parameters for 2024-T3 and 7075-T6 aluminum alloys are summarized in Table 1.

Several investigators have assumed that the crack growth rate in metallic materials is lognormal-distributed (e.g., citations in Sobczyk and Spencer, 1992). Some others have treated the crack length to be lognormal-distributed (e.g., Ray and Tangirala, 1997) based on the assumption that the crack growth process is highly correlated. The results of K-L expansion in Eqs. (12) to (17) are in agreement with these claims because  $\Omega(\zeta, \Delta S)$  which dominates the random behavior of fatigue crack growth can be considered as a perfectly correlated random process whereas the white noise  $\rho(\zeta, t)$  is a perfectly uncorrelated random process. Yang and Manning (1996) have presented an empirical second order approximation of crack growth by postulating lognormal distribution of a parameter

that does not bear any physical relationship to  $\Delta S$  but it is, to some extent, similar to  $\Omega(\zeta, \Delta S)$  in the present model.

We hypothesize that the random process  $\Omega(\zeta, \Delta S)$  is two-parameter ( $r = 2$ ) lognormal-distributed (Bogdonoff and Kozin, 1985) and its goodness of fit is examined by both  $\chi^2$  and Kolmogorov-Smirnov tests of experimental data. Each of the four data sets is partitioned into  $L = 12$  segments to assure that each segment contains at least 5 samples. With  $(L - r - 1) = 9$  degrees of freedom, the  $\chi^2$ -test shows that, for each of the four data sets, the hypothesis of two-parameter lognormal-distribution of  $\Omega(\zeta, \Delta S)$  passed the 10% significance level which suffices the conventional standard of 5% significance level. For each of the four data sets, the hypothesis of two-parameter lognormal-distribution of  $\Omega(\zeta, \Delta S)$  also passed the 20% significance level of the Kolmogorov-Smirnov test.

Next we hypothesize a probability distribution of  $\rho(\zeta, t)$ . Since the crack length and crack growth rate are guaranteed to be non-negative, Eq. (3) enforces that the random noise  $\rho(\zeta, t)$  must also be non-negative with probability 1 for all  $t$ . As a viable option, one may hypothesize the two-parameter lognormal distribution for  $\rho(\zeta, t)$  similar in structure to that of  $\Omega(\zeta, \Delta S)$ . Then, the right-hand side of Eq. (4) becomes lognormal-distributed because the product of two lognormal variables is lognormal. This makes the rate of fatigue crack damage (see Eqs. (4) and (8)) lognormal distributed.

**2.3 Model Prediction.** Figure 1 compares the analytically derived lognormal-distributed probability density functions (pdf's) of  $\Omega(\zeta, \Delta S)$  with the corresponding histograms generated from experimental data by approximately compensating the relatively small second-order statistics of the noise  $\rho(\zeta, t)$ . Referring to Table 1, the mean  $\mu_\Omega$  in the model is identical for the three data sets of 7075-T6 while the corresponding variance is different in each set. This is because  $\sigma_\Omega^2(\Delta S)$  is inversely proportional to  $(\Delta S)^{2m}$  and  $\Delta S$  is different for each data set— $\sigma_\Omega^2$  is largest for the Ghonem data set #3 for which  $\Delta S = 13.24$  MPa is smallest and  $\sigma_\Omega^2$  is smallest for the Ghonem data set #2 for which  $\Delta S = 17.80$  MPa is largest of the three data sets. However, for 2024-T3, no such comparison could be made because only one  $\Delta S$  is available in the Virkler data set.

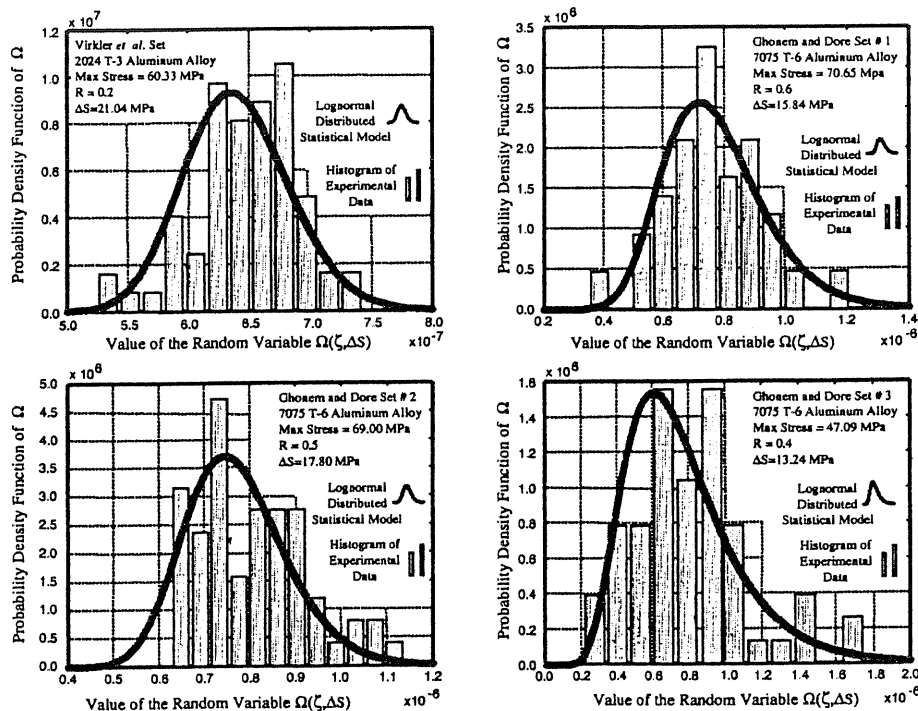


**Fig. 1 Identification of probability density function of the model parameter  $\Omega$**

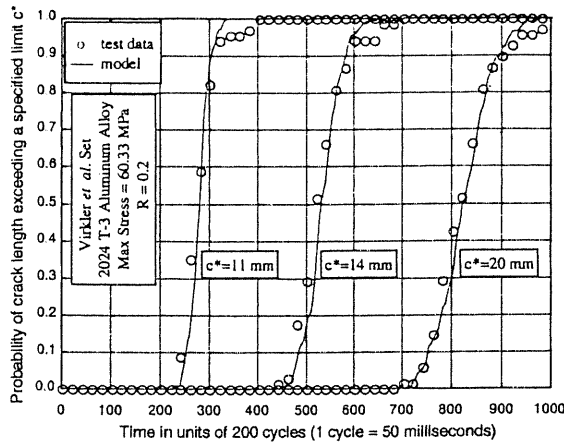


Fig. 2 Probability distribution of crack length exceeding specified limits (Virkler et al. data)

Model predictions of crack growth are now obtained by Monte Carlo simulation of the stochastic difference Eq. (3) using the parameters listed in Table 1. Lognormal distributions of both  $\Omega(\zeta, \Delta S)$  and  $\rho(\zeta, t)$  are realized by taking exponentials of outputs of the standard normal random number generator with different seed numbers. Both test data and model predictions are used to generate probability distribution functions (PDF's) of service cycles to exceed specified limits,  $c^*$ , of crack length. Note that the Virkler set and each of the three Ghonem sets contain 68 samples and 60 samples, respectively, while the Monte Carlo simulations for model prediction have been conducted with 1000 samples in each case. The PDF plots in Fig. 2 compare model predictions with the experimental data of Virkler et al. (1979) for three different values of  $c^*$  at 11 mm, 14 mm, and 20 mm. Similarly, the three PDF plots from left to right in Fig. 3 compare model predictions with the data sets, #2, #1, and #3 (in the decreasing order of the effective stress range  $\Delta S$ ), respectively, of Ghonem and Dore (1987) at  $c^* = 11$  mm. The agreement of the predicted PDF's in Figs. 2 and 3 with the respective experimental data is a consequence of fitting the key model parameter  $\Omega(\zeta, \Delta S)$  to a high level of statistical significance as seen in Fig. 1. The small differences between the model-based and experimental PDF's in Figs. 2 and 3 should be further reduced for larger ensemble size of the data sets as the histograms of  $\Omega(\zeta, \Delta S)$  in Fig. 1 would more closely fit the (right hand) tails of the probability density function (pdf) plots.

### 3 Risk Analysis and Remaining Life Prediction

This section illustrates how the stochastic model can be used for risk analysis and remaining life prediction of critical components.

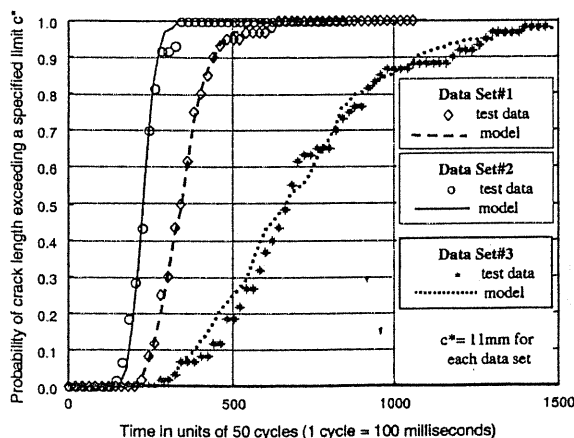


Fig. 3 Probability distribution of crack length exceeding a specified limit (Ghonem and Dore data)

As pointed out earlier, the impact of  $\rho(\zeta, t)$  on overall scatter of the crack growth profile is not significant for large  $(t - t_o)$ . In general,  $t_o$  signifies the starting time of a machine after maintenance and/or inspection. Since risk analysis and life prediction become important after a significant lapse of time (i.e., when  $(t - t_o)$  is sufficiently large), it is reasonable to make these decisions based only on the probability distribution function (PDF) of  $\Omega(\zeta, \Delta S)$ . Note that the error due to ignoring the effects of  $\rho(\zeta, t)$  is on the order of  $\sum_{j=2}^M \lambda_j / \sum_{j=1}^M \lambda_j$  that is in the range of 0.018 to 0.035 for all four sets as stated earlier in Section 2.

**3.1 Hypotheses Testing for Risk Analysis.** Let  $(M + 1)$  hypotheses be defined based on a partition of the crack length in the range  $[\bar{c}_o, \infty)$  where  $\bar{c}_o$  is the (known) minimum threshold of the initial crack length  $c(\zeta, t_o)$  which is assumed to be measured with good precision, i.e.,  $\sigma_{c_o}^2 \approx 0$ . The first  $M$  hypotheses are defined on the range  $[\bar{c}_o, \bar{c}_M)$  where  $\bar{c}_M$  is the critical crack length beyond which the crack growth rate rapidly becomes very large leading to complete rupture:

$$\begin{aligned} H_0(t, t_o): & c(\zeta, t) \in [\bar{c}_o, \bar{c}_1) \\ H_1(t, t_o): & c(\zeta, t) \in [\bar{c}_1, \bar{c}_2) \\ & \vdots \\ H_{M-1}(t, t_o): & c(\zeta, t) \in [\bar{c}_{M-1}, \bar{c}_M) \end{aligned}$$

$$\text{where } \bar{c}_i = \bar{c}_o + i \frac{(\bar{c}_M - \bar{c}_o)}{M}, \quad i = 1, 2, \dots, (M - 1) \quad (21)$$

The last (i.e., the  $M$ th) hypothesis is defined as  $H_M: c_r \in [\bar{c}_M, \infty)$  which is popularly known as the unstable crack region in the fracture mechanics literature (Suresh, 1991). Each of these  $(M + 1)$  hypotheses represents a distinct range in the entire space of crack lengths from an initial value till rupture occurs, and together, they form an exhaustive set of mutually exclusive regions in the state space of crack length. The first  $M$  hypotheses are generated as:

$$c(\zeta, t) \in H_j(t, t_o) = [\bar{c}_j, \bar{c}_{j+1}) \Rightarrow \psi(\zeta, t; t_o) [\psi_j, \psi_{j+1}) \quad \text{for } j = 0, 1, 2, \dots, M - 1 \quad \text{and a given } \Delta S \quad (22)$$

where  $\psi_j \equiv ((\bar{c}_j/w)^{1-m/2} - (\bar{c}_o/w)^{1-m/2}) / (1 - m/2) - m(\pi/4)^2 ((\bar{c}_j/w)^{3-m/2} - (\bar{c}_o/w)^{3-m/2}) / (3 - m/2)$  follows the structure of Eq. (7). As discussed earlier, the process  $\psi(\zeta, t; t_o)$  is approximated by ignoring the effects of the noise term  $(\rho(\zeta, t) - 1)$ , i.e., by setting the integral within parentheses on the right side of Eq. (8) to zero as:

$$\psi(\zeta, t; t_o) \approx w^{m-2} \Omega(\zeta, \Delta S) (\Delta S)^m (t - t_o) \quad (23)$$

Now the probability that the  $j$ th hypothesis,  $H_j(t, t_o)$ , can be obtained from the instantaneous (conditional) probability distribution function  $F_{\psi(c(\zeta, t_o))}(\cdot; t|\bar{c}_o)$  of  $\Psi(\zeta, t; t_o)$ . This is directly generated from the two-parameter lognormal distribution of  $\Omega(\zeta, \Delta S)$  without any computationally expensive integration because conversion of the range of integration in the log scale allows evaluation of the error function via table-lookup. These details are straight-forward and are not presented in this paper. Probabilities of the individual hypotheses become:

$$\begin{aligned} P[H_j(t, t_o)] &= F_{\psi(c(\zeta, t_o))}(\Psi_{j+1}; t|\bar{c}_o) - F_{\psi(c(\zeta, t_o))}(\Psi_j; t|\bar{c}_o) \\ &\quad \text{for } j = 0, 1, 2, \dots, M - 1 \\ P[H_M(t, t_o)] &= 1 - \sum_{j=0}^{M-1} P[H_j(t, t_o)] \end{aligned} \quad (24)$$

To elucidate the concept of hypothesis testing for risk analysis and life prediction, we present examples based on Virkler and Ghonem data sets. The probability that the random crack length  $\{c(\zeta, t); t \geq t_o\}$  at a given time,  $t$ , is located in one and only one of these segments is computed in real time by Eq. (24). For each

Table 2 Crack damage hypotheses for Virkler et al. data

Description	Range of Fatigue Crack Length
Hypothesis H <sub>0</sub>	9.00 mm ≤ c(t) < 12.6 mm
Hypothesis H <sub>1</sub>	12.6 mm ≤ c(t) < 16.2 mm
•	•
•	•
•	•
Hypothesis H <sub>9</sub>	41.4 mm ≤ c(t) < 45.0 mm
Hypothesis H <sub>10</sub>	45.0 mm ≤ c(t) < 76.2 (Unstable Crack Growth)

data set, it is observed that  $\bar{c}_0 = 9.0$  mm with probability 1. The critical crack length is chosen based on the geometry of the test specimens: For the Virkler experiment (in which the specimen

Table 3 Crack damage hypotheses for three sets of Ghonem and Dore data

Description	Range of Fatigue Crack Length
Hypothesis H <sub>0</sub>	9.00 mm ≤ c(t) < 10.8 mm
Hypothesis H <sub>1</sub>	10.8 mm ≤ c(t) < 12.6 mm
•	•
•	•
•	•
Hypothesis H <sub>9</sub>	25.2 mm ≤ c(t) < 27.0 mm
Hypothesis H <sub>10</sub>	27.0 mm ≤ c(t) < 50.4 (Unstable Crack Growth)

half-width is 76.2 mm).  $\bar{c}_w = 45.0$  mm, for the Ghonem experiments (in which the specimen half-width is 50.4 mm),  $\bar{c}_w = 27.0$  mm. The space  $[\bar{c}_w, w)$  is partitioned into  $(M + 1)$  regions. In these examples, we have chosen 11 hypotheses (i.e.,  $M = 10$ ) for both Virkler and Ghonem data sets. The range of each hypothesis is defined as depicted in Table II and Table III, respectively. The time evolution of probability of the hypotheses for the four data sets is shown in the four plates of Fig. 4. In each case, the plot of  $H_0$  begins with a probability equal to 1 at time  $t = t_0$  and later diminishes as the crack grows with time (i.e., number of load cycles applied). The probability of each of the hypotheses  $H_1$  to  $H_9$  is initially zero and then increases to a maximum and subsequently decreases as the crack growth process progresses with time. The probability of the last hypothesis  $H_{10}$  (on the extreme right in each plate of Fig. 4) of unstable crack growth beyond the critical crack length,  $\bar{c}_w$ , initially remains at zero and increases rapidly only when the specimen is close to rupture. At this stage, the probability of each of the remaining hypotheses is zero or rapidly diminishes to zero.

The hypotheses testing procedure can be executed in real time on inexpensive platforms such as a Pentium processor in the plant instrumentation and control system for issuing alerts and warnings while the machine is in operation. For example, the space of crack length, defined by  $[\bar{c}_w, w)$ , can be partitioned into four hypotheses denoting three regions of green, yellow and red alert conditions for the first three hypotheses and catastrophic conditions for the fourth hypothesis. While alerts and warnings are useful for operational support and safety enhancement, operations planning and maintenance scheduling require remaining life prediction. Equipment readiness assessment and failure prognosis based on current condition and projected usage of the machinery are important tools for operations and maintenance planning, especially in an information-based maintenance environment where access to all pertinent information is enabled.

**3.2 Remaining Life Prediction.** Having known the instantaneous (conditional) probability distribution function  $F_{\psi(\zeta, t, t_0)}(\cdot; t_{\zeta_0})$  of  $\Psi(\zeta, t, t_0)$ , the remaining life  $T(t, Y_d(t), \epsilon)$  can be computed on-line at any specified time instant,  $t$ , based on a desired plant

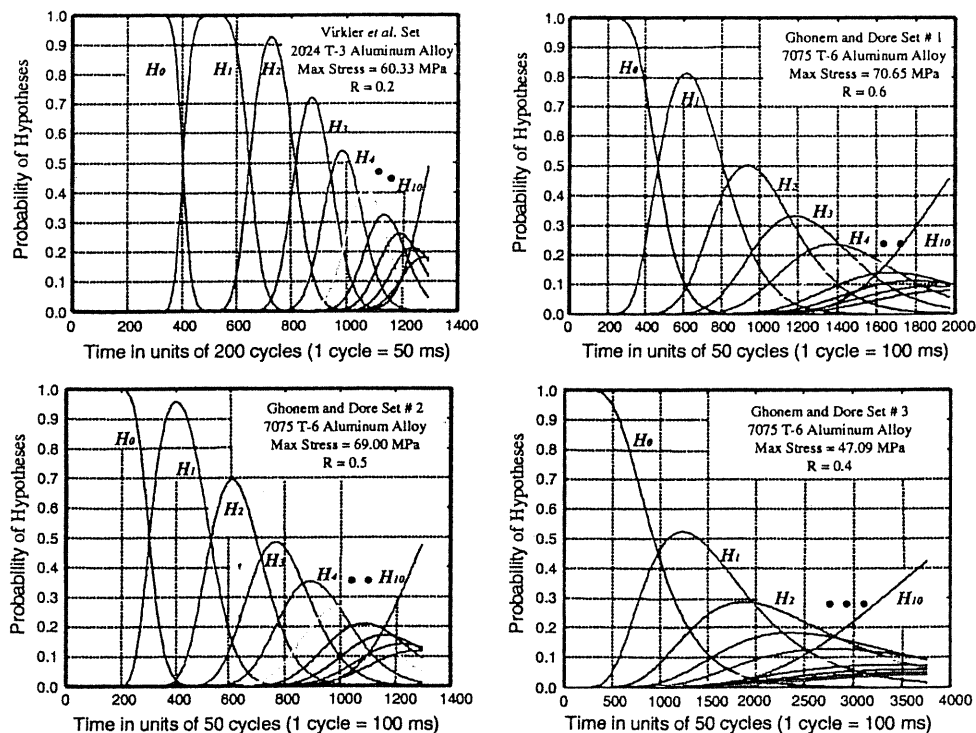


Fig. 4 Probabilities of hypotheses for fatigue crack propagation

operational profile  $Y_d(t) = \{y(\theta): \theta \geq t\}$  and a confidence level  $(1 - \epsilon)$ . This implies that if the plant operation is scheduled to yield the desired output  $Y_d(t)$ , then  $T(t, Y_d(t), \epsilon)$  is the maximum time of operation such that the probability of the crack length  $c(\zeta, t + T)$  to exceed  $\bar{c}_M$  is less than  $\epsilon$ . The algorithm for prediction of remaining life is obtained as:

$$T(t; Y_d(t); \epsilon) = \text{Sup} \{ \theta \in [0, \infty): P[c_{t+\theta} \leq \bar{c}_M] > (1 - \epsilon) \} \quad (25)$$

The prediction algorithm in Eq. (25) is executed in real time based on the current information. The generated results can then be conveyed to a decision making module (for example, a discrete-event supervisor, (Garcia and Ray, 1996; Zhang et al., 1999) at a higher level for failure prognosis, life extending control, and maintenance scheduling, or simply for generation of warnings and alerts. These results may also be displayed as a decision support tool for human operators. The objective is to determine the statistical confidence with which plant operations can be planned for a specified period of time or to evaluate alternate operational scenarios. This is also of considerable importance in the scheduling of maintenance to avoid untimely shutdowns since failure prognostic information is inherent in remaining life prediction. Some of these issues have been addressed by Ray and Tangirala (1996) and Ray et al. (1998).

#### 4 Summary and Conclusions

This paper presents a stochastic model of fatigue crack damage for risk analysis and life prediction of metallic structures and machinery components in mechanical systems (e.g., aircraft, spacecraft, and power plants). The fatigue crack damage at an instant (i.e., at the end of a stress cycle) is expressed as a continuous function of the current crack length and initial crack length. The uncertainties in the measure of crack damage accrue primarily from a single lognormal-distributed random parameter associated with individual specimens and, to a much lesser extent, from the random noise due to material inhomogeneity. This conclusion is consistent with the findings of other investigators.

The constitutive equation of the damage model is based on the physics of fracture mechanics and is validated by Karhunen-Loève analysis of fatigue test data for 2024-T3 and 7075-T6 aluminum alloys at different levels of (constant-amplitude) cyclic load. A systematic procedure for parameter identification is also established. The predicted probability distribution function (PDF) of service cycles to exceed a specified crack length is shown to be in close agreement with that generated from the test data. The (non-stationary) probability distribution function of crack damage is obtained in a closed form without numerically solving stochastic differential equations in the Wiener integral or Itô integral setting. The model allows formulation of risk assessment and life prediction algorithms for real-time execution on inexpensive platforms such as a Pentium processor. Examples are presented to illustrate how this stochastic model can be used to generate and update hypotheses of crack damage under constant-amplitude loading. Extension of the stochastic model to varying-amplitude deterministic and random loading is a subject of current research (Ray and Patankar, 1999). A unified model that accounts for different sources of uncertainties in crack growth needs to be established before practical applications become viable.

Potential applications of the stochastic model of fatigue crack damage include the following technologies: (i) life extending control (also referred to as damage-mitigating control) of mechanical systems (Kallappa et al., 1997; Holmes and Ray, 1998); (ii) analytical measurements and intelligent sensing (including real-time nondestructive evaluation) of fatigue crack damage; (iii) remaining life prediction of machinery components as well as generation of alerts and warnings for operational support and safety enhancement; and (iv) real-time maintenance decisions based on the information of machinery operation and anticipated usage.

#### Acknowledgments

The author is grateful to Professor B. M. Hillberry of Purdue University and Professor H. Ghonem of University of Rhode Island for providing the test data of random fatigue crack growth.

#### References

- T. L. Anderson, 1995, *Fracture Mechanics*, 2nd ed., CRC Press, Boca Raton, FL.
- V. V. Bolotin, 1989, *Prediction of Service Life for Machines and Structures*, ASME Press, New York.
- J. L. Bogdanoff, and F. Kozin, 1985, *Probabilistic Models of Cumulative Damage*, Wiley, New York.
- F. Casciati, P. Colombi, and L. Farvelli, 1992, "Fatigue Crack Size Probability Distribution via a Filter Technique," *Fatigue & Fracture of Engineering Materials & Structures*, Vol. 15, No. 5, pp. 463-475.
- O. Ditlevsen, 1986, "Random Fatigue Crack Growth—A First Passage Problem," *Engineering Fracture Mechanics*, Vol. 23, No. 2, pp. 467-477.
- K. Fukunaga, 1990, *Introduction to Statistical Pattern Recognition*, 2nd ed., Academic Press, Boston.
- H. E. Garcia and A. Ray, 1996, "State-space Supervisory Control of Reconfigurable Discrete Event Systems," *International Journal of Control*, Vol. 63, No. 4, pp. 767-797.
- H. Ghonem and S. Dore, 1987, "Experimental Study of the Constant Probability Crack Growth Curves under Constant Amplitude Loading," *Engineering Fracture Mechanics*, Vol. 27, pp. 1-25.
- M. Holmes and A. Ray, 1998, "Fuzzy Damage Mitigating Control of Mechanical Structures," *ASME JOURNAL OF DYNAMIC SYSTEMS, MEASUREMENT, AND CONTROL*, Vol. 120, No. 2, pp. 249-256.
- F. K. Ibrahim, J. C. Thompson and T. H. Topper, 1986, "A Study of the Effect of Mechanical Variables on Fatigue Crack Closure and Propagation," *International Journal of Fatigue*, Vol. 8, No. 3, pp. 135-142.
- H. Ishikawa, A. Tsurui, H. Tanaka, and H. Ishikawa, 1993, "Reliability Assessment Based Upon Probabilistic Fracture Mechanics," *Probabilistic Engineering Mechanics*, Vol. 8, pp. 43-56.
- A. H. Jazwinski, 1970, *Stochastic Processes and Filtering Theory*, Academic Press, New York.
- P. T. Kallappa, M. Holmes and A. Ray, 1997, "Life Extending Control of Fossil Power Plants for Structural Durability and High Performance," *Automatica*, Vol. 33, No. 6, pp. 1101-1118.
- P. E. Kloeden, and E. Platen, 1995, *Numerical Solution of Stochastic Differential Equations*, Springer-Verlag, Berlin.
- V. H. Kogajev, and S. H. Liebiedinskij, 1983, "Probabilistic Model for Fatigue Crack Growth," *Machinovedienije*, Vol. 4, pp. 78-83 (in Russian).
- Y. K. Lin, and Yang, J. N., 1985, "A Stochastic Theory of Fatigue Crack Propagation," *AIAA Journal*, Vol. 23, No. 1, pp. 117-124.
- J. C. Newman, Jr., 1984, "A Crack Opening stress Equation for Fatigue Crack Growth," *International Journal of Fracture*, Vol. 24, pp. R131-R135.
- S. Ozekici, ed., 1996, *Reliability and Maintenance of Complex Systems*, NATO Advanced Science Institutes (ASI) Series F: *Computer and Systems Sciences*, Vol. 154, Berlin, Germany.
- P. C. Paris and F. Erdogan, 1963, "A Critical Analysis of Crack Propagation Laws," *ASME Journal of Basic Engineering*, Vol. 85, pp. 528-534.
- R. Patankar, A. Ray, and A. Lakhtakia, 1998, "A State-Space Model Of Fatigue Crack Dynamics," *International Journal of Fracture*, Vol. 90, No. 3, pp. 235-249.
- A. Ray and S. Tangirala, 1996, "Stochastic Modeling of Fatigue Crack Dynamics for On-line Failure Prognostics," *IEEE Trans. Control Systems Technology*, Vol. 4, No. 2, July, pp. 443-451.
- A. Ray, and S. Tangirala, 1997, "A Nonlinear Stochastic Model of Fatigue Crack Dynamics," *Probabilistic Engineering Mechanics*, Vol. 12, No. 1, pp. 33-40.
- A. Ray, S. Phoha and S. Tangirala, 1998, "Stochastic Modeling of Fatigue Crack Propagation," *Applied Mathematical Modelling*, Vol. 22, pp. 197-204.
- A. Ray, and R. Patankar, 1999, "Stochastic Modeling Fatigue Crack Propagation under Variable Amplitude Loading," *Engineering Fracture Mechanics*, Vol. 62, pp. 477-493.
- J. Schijve, 1976, "Observations on the Prediction of Fatigue Crack Growth Propagation Under Variable-Amplitude Loading," *Fatigue Crack Growth Under Spectrum Loads*, ASTM STP 595, pp. 3-23.
- K. Sobczyk, and B. F. Spencer, 1992, *Random Fatigue: Data to Theory*, Academic Press, Boston, MA.
- B. F. Spencer, J. Tang, and M. E. Artley, 1989, "A Stochastic Approach to Modeling Fatigue Crack Growth," *The AIAA Journal*, Vol. 27, No. 11, pp. 1628-1635.
- S. Suresh, 1991, *Fatigue of Materials*, Cambridge University Press, Cambridge, UK.
- A. Tsurui, and H. Ishikawa, 1986, "Application of the Fokker-Planck to a Stochastic Fatigue Growth Model," *Structural Safety*, Vol. 4, pp. 15-29.
- D. A. Virkler, B. M. Hillberry, and P. K. Goel, 1979, "The Statistical Nature of Fatigue Crack Propagation," *ASME Journal of Engineering Materials and Technology*, Vol. 101, No. 2, pp. 148-153.
- E. Wong, and B. Hajek, 1985, *Stochastic Processes in Engineering Systems*, Springer-Verlag, New York.
- J. N. Yang, and S. D. Manning, 1996, "A Simple Second Order Approximation of Stochastic Crack Growth Analysis," *Engineering Fracture Mechanics*, Vol. 53, No. 5, pp. 677-686.
- H. Zhang, A. Ray and S. Phoha, 1999, "Hybrid Life Extending Control of Mechanical Structures: Experimental Validation of the Concept," *Automatica*, to appear.